Relating cortical potentials to scalp EEG's in a realistically shaped inhomogeneous head model by means of the boundary element method

Y. Fan[1], T. Jiang[1,2], and X. Li[1]

[1]*National Laboratory of Pattern Recognition, Institute of Automation, Chinese Academy of Sciences, 100086 Beijing, China;* [2]*School of Computer Science, The Queen's University of Belfast, Belfast BT7 1NN, UK*

1 Introduction

A central problem in EEG is to efficiently solve the inverse problem. It consists of the estimation of location, orientation, and strength of the current sources in the brain with the measurements of the electric potential on the surface of the head. In order to solve this problem, we have to first obtain the solution of the forward problem, i.e., the calculation of the electric potential due to known current sources in a specified conducting volume. To this end, a variety of efficient methods have been developed. The most remarkable one of the existing methods is directly estimating potential at the superficial cerebral cortical surface from EEG recordings on the scalp with the boundary element method (BEM) in a realistically shaped inhomogeneous head model. It has made great improvement in spatial resolution [1]. Compared to other methods, the cortical potential imaging approach provides a powerful imaging means and a much-enhanced spatial resolution in assessing the underlying brain activity without modeling the electrically activated brain regions by current dipoles.

In such a method, the BEM is used to account for a realistically shaped inhomogeneous head that consists of various compartments of the head, e.g., brain, skull, and scalp, as they can be determined from Magnetic Resonance Images (MRI's). It is well known that the BEM is an effective approach for calculating the forward solution. The factors affecting the accuracy of the BEM in the forward problem were studied by many researchers. Their studies demonstrated that the choice of basis functions, density of elements, and shape of each element are essential for the accuracy of BEM in the forward problems [3-5]. Though a higher element density can provide a more accurate representing surface and a more accurate solution, element density is limited by physical technique. The choice of shapes of elements is most often confined to flat triangular element due to its simplicity in the mathematical formulation of the problem and its capability to approximate any complex surface. However, the choice of basis functions is free of the physical constraint. The dominant choice is constant basis functions due to its simplicity. However, in this case, the numerical errors also are very high unless the element density is highly increased, but this will result in extensive computation time and storage demands. A better choice is linear basis functions. This is because in this case, the number of equations can be reduced about a half of that in the case of constant basis functions, and the accuracy has not decreasing in the same rate [3]. An interesting problem is if there exists a more suitable choice for basis functions choice. This paper addresses this problem.

In this paper, we present a new approach by means of BEM based on natural element interpolation [2,8,9] that established a more direct and accurate relation between cortical potential and scalp potential. The natural-neighbor coordinate is extended so that it can be used in triangular element. Furthermore, the equations we established are directly related to nodes rather than triangles, which can reduce the computational cost and improve computational accuracy. In order to validate our method, we also conducted computer simulations based on a concentric three-shell head model.

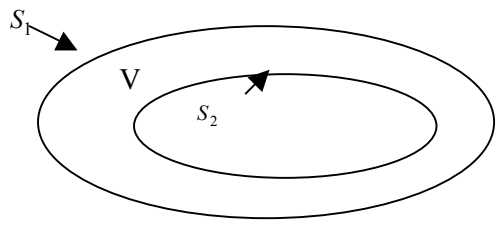

Fig.1 *Volume V surrounded Surface S.* $S = S_1 \cup S_2$

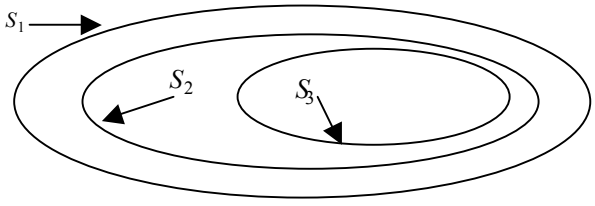

Fig.2 *A three-shell volume conductor model. The volume between* S_1 *and* S_2 *is denoted as* V_1*, and that between* S_2 *and* S_3 *is denoted as* V_2*.*

2 Methods

2.1 Integral Equations

Applying Green's second identity to an isotropic homogeneous volume conductor, we have [8]

$$-2\pi u(\mathbf{r}\in\mathbf{S})=\int_V \frac{1}{r}\nabla^2 u(\mathbf{r})dV+\int_S\left[u(\mathbf{r})\nabla\frac{1}{r}-\frac{1}{r}\nabla u(\mathbf{r})\right]\bullet d\mathbf{S} \quad (1)$$

where u is the potential, $\mathbf{r}$ is the vector from observer point to source point, $r=|\mathbf{r}|$, and V is the volume inside the surface as shown in Fig.1. When no current source exists between the surfaces, $\nabla^2 u=0$. Therefore, we have

$$-2\pi u(\mathbf{r}\in\mathbf{S})=\int_S\left[u(\mathbf{r})\nabla\frac{1}{r}-\frac{1}{r}\nabla u(\mathbf{r})\right]\bullet d\mathbf{S} \quad (2)$$

For convenience, we modify (2) to

$$u(\mathbf{r})=-\frac{1}{2\pi}\int_S u\bullet d\Omega+\frac{1}{2\pi}\int_S\frac{1}{r}\bullet\frac{\partial u}{\partial r_n}dS \quad (3)$$

where u is the potential on the point $\mathbf{r}$ and $\mathbf{r}\in S_1\cup S_2$, $d\Omega=\frac{\mathbf{r}\cdot\mathbf{r_n}}{r^2}dS$, $r=|\mathbf{r}|$, $\mathbf{r_n}$ is an outward pointing vector of unit magnitude normal to surface element dS.

Our knowledge on the conductivity of the brain tissue is very limited, which makes us have to assume that the head consists of a number n of disjoint homogeneous regions $V_1,\cdots,V_n$ with boundaries $S_1=\partial V_1,\cdots,S_n=\partial V_n$. Those regions are volume conductors with constant conductivity respectively, which are usually chosen to be the scalp, skull, cerebrospinal fluid, gray matter and white matter. In this paper, we only consider a three-shell head model that consists of scalp, skull and brain, respectively, as Fig.2. So scalp V_1 is bounded by a surface $S=S_1\cup S_2$, skull V_2 is bounded by a surface $S=S_2\cup S_3$, and brain V_3 is bounded by a surface S_3.

Since no current sources exist in volume V_1 (scalp) and $\nabla u(r)=0$, $r\in S_1$, by applying (3) to it and by locating the observed point on S_1 or S_2, we can get

$$u(\mathbf{r})=-\frac{1}{2\pi}\int_{S_1}ud\Omega+\frac{1}{2\pi}\int_{S_2}ud\Omega-\frac{1}{2\pi}\int_{S_2}\frac{1}{r}\frac{\partial u}{\partial\mathbf{r_n}}dS. \quad (4)$$

By discretizing the surfaces S_1 and S_2 into triangle elements (TE's), we get the discretization points that are the triangles' vertices, and from (4) we have

$$\begin{aligned}u_i^k=&-\frac{1}{2\pi}\sum_{j=1}^{N_1}\int_{\Delta_j^1}ud\Omega+\frac{1}{2\pi}\sum_{j=1}^{N_2}\int_{\Delta_j^2}ud\Omega\\&-\frac{1}{2\pi}\sum_{j=1}^{N_2}\int_{\Delta_j^2}\frac{1}{r}\frac{\partial u}{\partial\mathbf{r_n}}dS\\&i=1,\ldots,N_k,\ k=1,2,\end{aligned} \quad (5)$$

where u_i^k is the potential on jth discrete point on surface S_k, $r=|\mathbf{r}|$.

Δ_j^k is the jth triangular element belonging to the surface S_k.

Assuming $\{h_n(\mathbf{r})\}_{n=1}^N$ is a set of basis functions and $\{\mathbf{r}_m\}_{m=1}^N$ is a set of discretization points on S_1 or S_2, we can get

$$h_n(\mathbf{r}_m)=\delta_{nm}. \quad (6)$$

Then the unknown potential $u(\mathbf{r})$ can be expanded in terms of $h_n(\mathbf{r})$:

$$u(\mathbf{r})=\sum_{n=1}^N u_n h_n(\mathbf{r}). \quad (7)$$

By applying (7) to (5), we get

$$\begin{aligned}u_1^i=&-\frac{1}{2\pi}\sum_{j=1}^{N_1}\sum_{i=l,m,n}u_i\int_{\Delta_j^1}h_i(\mathbf{r})d\Omega\\&+\frac{1}{2\pi}\sum_{j=1}^{N_1}\sum_{i=l,m,n}u_i\int_{\Delta_j^2}h_i(\mathbf{r})d\Omega\\&-\frac{1}{2\pi}\sum_{j=1}^{N_1}\int_{\Delta_j^2}\frac{1}{r}ds\sum_{i=l,m,n}u_i\frac{\partial h_i}{\partial\mathbf{r_n}}\end{aligned} \quad (8)$$

Combining the left-hand side of (8) with the first term in the right-hand side of (8), and rewriting in matrix format, we get

$$P_{11}U_1+P_{12}U_2+G_{12}U_2=0 \quad (9)$$

where U_k is the column vector consisting of potentials at every vertices of triangular element of S_k and P_{11},P_{12},G_{12} are coefficient matrices with dimensions of N_1 by N_1, N_1 by N_2 and N_1 by N_2, respectively.

$$p_{11}^{ij}=-\frac{1}{2\pi}\sum_{\Delta_k^1\in P_j^1}\int_{\Delta_k^1}h_j(\mathbf{r})d\Omega-\delta_{ij}, \quad (10)$$

$$p_{12}^{ij}=\frac{1}{2\pi}\sum_{\Delta_k^2\in P_j^2}\int_{\Delta_k^2}h_j(\mathbf{r})d\Omega, \quad (11)$$

$$G_{12}^{ij}=-\frac{1}{2\pi}\sum_{\Delta_k^2\in P_j^2}\frac{\partial h_j}{\partial\mathbf{r_n}}\int_{\Delta_k^2}\frac{1}{r}dS \quad (12)$$

where p_j^k={discrete point j contained within the *element* on S_k}.

Set the observer point on S_2, by the similar steps, we can get

$$P_{21}U_1 + P_{22}U_2 + G_{22}U_2 = 0\,, \qquad (13)$$

Apply (3) to the volume V_2 and locate the observe point on S_2 or S_3, we can get another two equations

$$P'_{22}U'_2 + P_{23}U_3 - G'_{22}U'_2 + G_{23}U_3 = 0\,, \qquad (14)$$

$$P'_{32}U'_2 + P_{33}U_3 + G'_{32}U'_2 + G_{33}U_3 = 0\,, \qquad (15)$$

where U'_2 is the column vector consisting of potentials at every vertices of triangular element of S_2 but just inside of V_2. The boundary condition on S_2 can be expressed as follow:

$$U'_2 = U_2\,. \qquad (16)$$

Due to the constraint of the number of sensors, we often set the number of the discrete point on surfaces S_2 and S_3 that are much greater than the number of sensors in order to get higher accuracy. In this case, the coefficient matrixes all are perhaps singular. Therefore, we cannot get unique solutions from (9), (13), (14), (15), and (16). Since this ambiguity can be removed by deflation [6,7], so we can derive the unique relationship between the potential on the surface S_1 and S_2, and that between the potential on the surface S_2 and S_3. The unique relations between scalp potential and skull potential and that between skull potential and cortical potential can be derived

$$U_2 = AU_1\,, \qquad (17)$$

$$U_3 = BU_2\,, \qquad (18)$$

From (17) and (18), we also have

$$U_3 = BAU_1 = TU_1\,. \qquad (19)$$

After the decision for the basis functions is made, we can get the potential distribution on the cortical surface from the potential distribution on the scalp. The simple basis functions have been studied by several authors such as constant potential and linear interpolation [1,3].

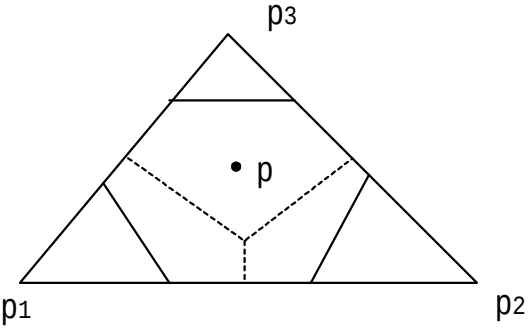

Fig.3 *Voronoi region of an additional point (situation without drawn dashed)*

2.2. Natural Neighbor interpolation: Natural neighbor interpolation was devised by Sibson, which is related to triangle based interpolation [9,10]. Here, we give an extension of it:

We confine the interpolation in a triangular plane whose three vertexes are the given data point, and the Voronoi tessellation is the decomposition of the triangular plane into the cells of the nearest neighbourhood of the three vertexes, shown as Fig.3. If S_i is the Voronoi proximal cell of data point $\mathbf{P_i}$ and $S(\mathbf{x})$ is the proximal cell of $\mathbf{x}$ in a Voronoi tessellation of the data points plus the point $\mathbf{P}$, then the volumes of the overlaps of $S(\mathbf{P})$ with the proximal cells S_i of the data points scaled by the volume of $S(\mathbf{P})$ give the local coordinate of $\mathbf{P}$ with respect to the data point $\mathbf{P_i}$:

$$h_i(\mathbf{P}) = \frac{v(S(\mathbf{P}) \cap S_i)}{v(S(\mathbf{P}))}\,. \qquad (20)$$

Therefore, the $h_i(\mathbf{P})$ can be used to determine an interpolation function

$$f(\mathbf{P}) = \sum_i h_i(\mathbf{P}) u_i\,. \qquad (21)$$

This function and its first derivatives are continuous everywhere except at the data points, which makes it ideally suited for our method. The expressions for natural neighour interpolation and its first derivatives have been derived by Sambridge etc. [10]. All the expressions have been used in this paper after a slight modification for our special case.

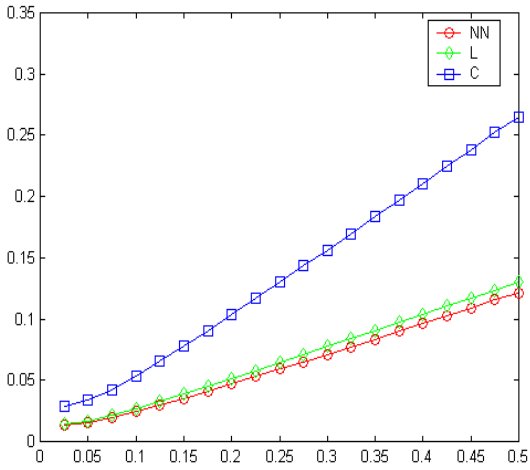

Fig.4 *Relative errors versus the eccentricity. The horizontal axis refers to the eccentricity of the dipole sources and the vertical axis refers to the relative error: NN refers to natural neighbor interpolation, L refers to linear interpolation, and C refers to constant potential method.*

3 Results

The accuracy of the present method was tested with a concentric three-shell sphere head model. The numerical solution was compared with the values given by analytical expressions. In the three-shell sphere head model, the radii were chosen to be 1.0, 0.92, and 0.87, respectively. The values of conductivity were chosen to be 1, 0.0125, and 1, respectively. Each surface of three-shell sphere was subdivided uniformly into 1642 triangles. The transmatrix T was calculated according (8)-(21).

Comparisons between the methods based on natural neighbor interpolation, linear interpolation, and constant potential are made in Fig.4. The dipole source was located at $(r \cdot \sin(\pi/4),\ 0,\ r \cdot \cos(\pi/4))$ with varying eccentricity r.

Our results have shown that a more accurate estimation cortical potential was gained even when the linear element interpolation was used.

4 Discussion

The method given in this paper can provide a means by which a direct relationship between the SP's and CP's can be established. Two highly significant practical advantages of this method are: 1) to formulate the equations in term of apexes instead of triangles. First, if each apex corresponds to an electrode, we can directly determine the equations for the apexes from experimental data. Second, the number of equations can be reduced about one-half and the accuracy can be greatly improved especially when an interpolation method of high quality was used. 2) Natural neighbor interpolation is local and the derivatives of the interpolated function are continuous everywhere except at the data points. These properties meet the need for high order continuous basis functions. Natural neighbor interpolation is better than quadratic interpolation since the latter requires additional nodes, besides those at the vertices of the triangles, e.g., at the midpoints of the sides of the triangles.

We did not fully investigate the extent to which the natural neighbor interpolation could be used to improve the accuracy of BEM, though the results have demonstrated that a high accuracy was achieved. The dominant shortcoming of using natural neighbor interpolation in BEM is that it is much slower in performance than linear interpolation. Therefore, our future work is to improve its algorithm implementation.

In summary, the experiment result and theory analysis show that our approach is very promising to further our capability of exploring the relation between the cortical potential and the scalp potential noninvasively.

Acknowledgements

This work was supported by the Natural Science Foundation of China, Grant No. 69705002, 697908001, and State Commission of Science and Technology of China, Grant No. G1998030503.

References

1. B. He, Y. Wang, and D. Wu, "Estimating cortical potential from scalp EEG's in a realistically shaped inhomogeneous head model by means of the boundary element method", *IEEE Trans. Biomed. Eng.* **46**, 1264–1268, 1999.
2. J. Braun and M. Sambridge, "A numerical method for solving partial differential equations on highly irregualr evolving grids", *Nature.* **376**, 655–660 (1995).
3. B.N. Cuffin, “Effects of head shape on EEG's and MEG's”, *IEEE Trans. Biomed. Eng.* **37,** 44-52,1990.
4. A.S.Ferguson and G. Stroink, "Factors affecting the accuracy of the boundary element method in the forward problem—I: calculating surface potentials", *IEEE Trans. Biomed. Eng.* **44**, 1139–1155, 1997.
5. J.W.H.Meijs, O.W. Weier, M.J.Peters, and A.Van Oosterom, "On the numerical accuracy of the boundary element method", *IEEE Trans. Biomed. Eng.* **36**, 1038–1049, 1989.
6. T.F. Chan, "Deflated decomposition of solutions of nearly singular systems", *SIAM J. Numer. Anal.*, **21**, 739–754,1984.
7. M.S. Lynn and W.P. Timlake, "The use of multiple deflations in the numerical solution fo singular systems of equations, with application to potential theory", *SIAM J. Numer. Anal.*, **5**, 303–322,1968.
8. A.C.L. Barnard, I.M. Duck, and M.S. Lynn, "The application of electromagnetic theory to electrocardiology: I. derivation of the integral equations", *Biophysical Journal*, **7**, 443–462, 1967.
9. H. Muller and D. Ruprecht, "Spatial interpolants for warping", in *Brain warping*, A.W. Toga, Academy Press, 1999, pp.199–220
10. M. Sambridge, J. Braun, and H. McQueen, "Geophysical parameterization and interpolation of irregular data using natural neighbours", *Geophys. J. Int.* **122,** 837–857,1999.